EXPERIMENTAL LIMITS ON NUCLEON DECAY AND $\Delta B = 2$ PROCESSES*

THE IMB COLLABORATION

T. W. Jones[2,7], R. M. Bionta[2], G. Blewitt[4], C. B. Bratton[5], B. G. Cortez[2,a], S. Errede[2], G. W. Foster[2,a], W. Gajewski[1], K. S. Ganezer[1], M. Goldhaber[3], T. J. Haines[1], D. Kielczewska[1,b], W. R. Kropp[1], J. G. Learned[6], F. Lehmann[4], J. M. LoSecco[4], H. S. Park[2], F. Reines[1], J. Schultz[1], E. Shumard[2], D. Sinclair[2], H. W. Sobel[1], J. L. Stone[2], L. R. Sulak[2], R. Svoboda[6], J. C. van der Velde[2], and C. Wuest[1].

(1) The University of California at Irvine
Irvine, California 92717

(2) The University of Michigan
Ann Arbor, Michigan 48109

(3) Brookhaven National Laboratory
Upton, New York 11973

(4) California Institute of Technology
Pasadena, California 91125

(5) Cleveland State University
Cleveland, Ohio 44115

(6) The University of Hawaii
Honolulu, Hawaii 96822

(7) University College
London, United Kingdom

I present results from the IMB proton decay detector based on 132 days of live-time. I go into some detail on how we calibrate the detector and what are background limitations of such a device. I hope we can stimulate some discussion of these technical points amongst the various representations of the other nucleon decay detectors who will give some of the following talks.

I begin with a basic description of how the detector works and how we calibrate it.

The IMB proton decay detector consists of a large rectangular volume of water located at a depth of 1670 mwe in a salt mine east of Cleveland, Ohio. The six surfaces of the volume are covered by 2048 (5 inch diameter) photomultiplier tubes (PMT) which detect Cherenkov light emitted by relativistic charged particles in the water. The distances between the tube planes in the E-W, N-S, and vertical directions are 22.8 m, 16.8 m, and 18.0 m, respectively. The fiducial volume begins 2.0 m in from the tube planes and contains 2.0×10^{33} nucleus, 1/9 of which are free protons.

*Presented by J. C. van der Velde at the Blacksburg Miniconference on Low Energy Tests of Conservation Laws in Particle Physics

0094-243X/84/1140001-16 $3.00

Filling the detector was completed on July 30, 1982 and useful data taking commenced in September. I will report on 132 days of live time taken prior to August 1, 1983.

OPERATION AND CALIBRATION OF THE DETECTOR

The detector is divided into 32 "patches" each consisting of 64 PMT. An event trigger consists of the time coincidence (within 120 ns) of any two patchs which themselves had a coincidence of $\geq$ 3 PMT in 60 ns. This "two patch" trigger is "OR-ed" with another trigger which consists of $\geq$ 12 PMT from the full detector in 60 ns. The trigger rate is 2.7/sec, virtually all due to atmospheric muons. The average dark noise in the tubes is 2.5 KHz with occasional tubes as high as 50 KHz. The number of noise triggers is negligible once the detector becomes dark adapted (a few hours after being exposed to light).

For each PMT which fires within $\pm$ 250 ns of the trigger time we record the time (T_1), the pulse height (Q), and whether or not the tube had a pulse (T_2) in a longer time scale running to 7.5 μsec after the trigger. The detector is calibrated using two different known sources of light: a "laser ball" situated in the center of the detector is driven by a 337 nm Nitrogen laser and emits isotropic bursts of light at various known times and known (relative) light levels. The absolute light-level, which is directly related to the energy of showering particles, is calibrated using single cosmic rays. These cosmic rays also tell us the absolute PMT efficiencies and give us measurements of light scattering and absorption in the water. Light absorption is also measured using the laser ball and in external test stands.

Figure 1 shows a schematic cross section of a single straight track passing through the detector. For $\beta = 1$ the Cherenkov cone of light is emitted at an angle of 41° with respect to the track. Successive isochronous wave fronts are shown emanating from the track as it traverses the detector. The arrival times and pulse heights allow us to reconstruct the track position and angle. From each hit PMT we can project back to the track and determine the flight path (D) and distance along the track (L) at which the photon was emitted, assuming that it was not scattered. Figure 2a shows the integrated pulse height (proportional to total photoelectron count) recorded as a function of L (in % of track length) for 150 computer simulated muons generated to enter and exit within 4 m radius circles centered at the top and bottom of the detector. The true entry points were chosen and then the track angles were reconstructed using the photoelectron (PE) weighted directions of the hit tubes. (This is our normal procedure for reconstructing track angles from a given vertex. It gives the correct direction to within 1° for these muons whose correct vertex has been assigned.) Note the sharp response function of the phototubes as the Cherenkov cone hits the side walls of the detector. The fact that the step-function of the Cherenkov cone is not flat is due to absorption in the water. Note especially the low (~ 1%) light intensity outside the Cherenkov cone. This shows the effect of knock-on electrons generated in the material preceding the detector and in the early part of the track's path through the water. There is no Rayleigh scattering included in the simulated events shown in Figure 2a. The effect of Rayleigh scattering can be seen in Figure 2b where we make a similar plot for a selected sample of real muons chosen to have entry and exit points similar to those of Figure 2a. This gives us a measure of the amount of Rayleigh

scattering we must put into the simulated ("Monte Carlo") events. The response function of the real events does not have quite as sharp a rise as the simulated events. We can reproduce this effect in the simulated events if we smear the entry points by about 2 m, consistent with our error in their determination.

Correction for water absorption of photons is a strong function of wave length (λ) and can only be done in an approximate way for each PMT hit since we don't measure λ. The light from near the beginning of the track (L = 0) has typically traveled through 20 m of water whereas that near the end of the exiting track has traveled only ~ 1 m. Our correction for water absorption over this difference in distance can be seen in Figure 2c where the response function now is approximately flat.

Another important piece of information we need in order to properly generate Monte Carlo events is the absolute efficiency of the PM tubes to respond to Cherenkov light generated by a single relativistic track and passed through a distance D of water. Starting with the known Cherenkov spectrum we must modulate it by water aborption and scattering, PMT glass transmission and photocathode response, and PMT single PE capture efficiency. We use our test-stand measurements of water absorption, our previously described value for Rayleigh scattering, the PMT manufacturer's (EMI) values for glass transmission and photocathode response, and 50% capture efficiency. This reproduces the efficiency vs D curve to within a few percent over the entire range D = 0 to 24 m, as can be seen in Figure 3.

The time jitter in the PM tubes can be measured "in situ" by analyzing pulses from the laser ball. If we calibrate the tubes with the ball in one position, and then move it to various other positions and reconstruct its location, the error in that reconstruction is a direct measure of our spatial resolution for a point source of light. It is important to understand this spatial resolution since this type of vertex reconstruction by time-of-flight is used extensively in rejecting background and calculating efficiencies for events which originate in the fiducial volume. Figure 4 shows that the spatial resolution for reconstructing a point source is ~ 50 cm. This is directly related to the time jitter in the tubes of ~ 11 ns (FWHM) at the single PE level. If we put the measured average time jitter (including pulse height slewing) into the Monte Carlo simulations we find that typical vertex error for back-to-back (or multibody) nucleon decays are ~ 60 cm. Events which give light mostly in one direction (e.g., the majority of atmospheric neutrino interactions and neutrino modes of nucleon decay) have spatial resolution of ~ 50 cm perpendicular to the track and ~ 150 cm along the track.

In summary, we now have all of the ingredients necessary in order to accurately simulate events:

-Track generation
This is straight forward in a homogeneous medium like water.

-Light generation
The simple β-dependent Cherenkov effect is used.

-Light scattering and absorption
These have been measured as discussed above.

-PMT efficiency
Measured in situ using cosmic rays.

-PMT time response
Measured using the laser ball.

-PMT pulse height to energy conversion
We are in the process of refining our conversion of pulse height to ionization energy. This is done initially in a relative way using neutral density filters in the laser system to linearize the Q response of each PMT. The absolute scale is then determined by cosmic rays. We estimate our present systematic uncertainty as ± 15%. This uncertainty has no significant effect on the conclusions presented in this paper.

DATA FILTERING

All of the 250,000 triggers per day taken in the mine are processed through three independent analysis chains. The first cut, which can be made before the events are written on tape, reduces the data by a factor of three. Subsequent cuts make use of the timing and geometrical properties of Cherenkov light to reject tracks entering the detector from the outside. The cuts are highly efficient for saving events which originate inside the fiducial volume, which starts two meters in from the tube planes. Typical efficiencies for a given filter are 80% - 90% for "wide angle" (light spread over more than a single hemisphere) events and 60% - 70% for "narrow angle" or single track events whose vertices are inside the fiducial volume. These efficiencies deteriorate as the number of lit tubes in the event decreases, so that normally a lower limit of 40 tubes is imposed on the data. This represents about 220 MeV for a showering track or ~ 450 MeV for a charged pion or muon. The number of lit tubes from some typical tracks is given in the following table.

TABLE I

Mean number of lit tubes from various tracks originating in the fiducial volume.

REACTION	PARTICLE	PARTICLE'S MEAN NO. OF PMT'S ($\pm\sigma$)
$N \to e\pi$	e	83 ± 15
$N \to eK$	e	58 ± 15
$N \to e\rho$	e	36 ± 10
$N \to \mu\pi$	μ	41 ± 10
$N \to \mu K$	μ	21 ± 7
$N \to \mu\Delta$	μ	34 ± 20
$N \to e\pi$	π°	87 ± 15
$N \to \mu K$, $K \to 2\pi$	π°	57 ± 18
$K^+ \to 2\pi$ at rest	π° π^+	57 ± 11 2.3 ± 1.5
$N \to \mu\pi$	$\pi^\pm$	29 ± 8
$N \to e\rho$, $\rho \to 2\pi$	$\pi^\pm$	18 ± 10
$\nu N \to l^\pm \Delta$, $\Delta \to N\pi$	$\pi^\pm$	42 ± 20
$\mu \to e\nu\bar{\nu}$	e	8 ± 4

It can be seen from the table that most nucleon decays comfortably pass the 40 tube cut (except for decays with charged kaons or neutrinos.) On the other hand, one also sees that individual tracks from several decay modes can frequently light fewer than 20 tubes. This makes positive identification difficult or impossible in some cases. (Typically one can identify at track which lights at least 20 tubes, or even 10 tubes if it is well isolated from other tracks.)

The upper limit on lit tubes is typically set at 300 tubes. One of the analysis chains goes up 500 tubes, but with reduced efficiency for exiting and down-going tracks. This upper limit allows us to study neutrino events, and anything else that might occur in the fiducial volume, up to an energy of ~ 3.5 GeV. (Higher energy neutrino events, from ~ 3 GeV to several hundred GeV, are recorded at the rate of 0.5/day by means of the upgoing muons that they generate outside the detector.)

The Cherenkov energy (E_c) distribution of 109 contained events taken from 132 days of live-time is shown in Figure 5. This is completely consistent with what one expects from atmospheric neutrino interactions in the detector, although the uncertainties in the expected values are large enough so that a

considerable fraction of the events we see could be due to other phenomena if the energy E_c were the only parameter we measured. (For example, a large number of events from an obstinate mode such as $p \to e^+\nu\nu$ could be hiding in Figure 5 and we would never know it.)

For most nucleon decay and $N\bar{N}$ annihilation modes the detector gives us more information than just the energy. In particular, for many modes we can measure the directions and energies of individual tracks. The criteria for this is that the track light up at least 10 tubes and that it be separated or distinguishable from other tracks. The 10-tube criterion corresponds to an energy threshold of ~ 50 MeV for showering tracks ($e^\pm$ or γ's) and 250 MeV and 315 MeV, respectively, for $\mu^\pm$ and $\pi^\pm$. (The additional threshold energy for charged tracks represents the energy at which their Cherenkov light yield falls below 50% of its maximum value.)

For some nucleon decay modes, like $e^+\pi^0$, $\mu^+\pi^0$, we will see two clearly separated tracks with an included angle of > 150°. For such events we have 3 parameters to work with: total energy, included angle, and energy ratio of the two tracks. These allow us to place strong constraints on the hypothesized decay and give us a large background rejection factor for neutrino induced events. Of course, one must also take into account degradation of the signal due to nuclear interactions of pions both inside the parent oxygen nucleus and in the water. These are quite severe for charged pions.

Some final states, such as $\mu^+(K^0 \to 2\pi^0)$, $\nu(K^0 \to 2\pi^0)$, $\mu^+(\eta^0 \to 3\pi^0, \gamma\gamma)$, and most $N\bar{N}$ annihilations, are not simple 2-body decays and yet they give significant Cherenkov light outside of a single hemisphere. For such modes it is convenient to define a parameter which measures the extent to which this happens. One such parameter is "Isotropy," which is defined as the summed unit vectors to all of the lit tubes from the assigned vertex divided by number of tubes. This variable will peak at 0.75 for a perfect Cherenkov ring of half angle 41° and be near zero for an isotropic or symmetric back-to-back event. The data from 132 days of live-time is shown on a scatterplot of E_c vs Isotropy in Figure 6. We see that the majority of events cluster around Isotropy = .7 indicating they are single-track-like. This plot, including the events at small Isotropy values, is consistent with what we expect from atmospheric neutrino interactions. The circled areas represent the region in which ~90% of the decays $p \to \mu^+(K^0 \to 2\pi^0)$ (dashed) and $N \to \nu(K^0 \to 2\pi^0)$ (solid) are expected to occur. By making further geometrical cuts on the events, and requiring a $\mu \to e$ decay where appropriate, we are able to reduce the events in the circled areas to 1 candidate for $p \to \mu^+K^0$ and 3 candidates for $N \to \nu K^0$. These residual candidates are consistent with nucleon decay to those modes but are also consistent with the neutrino background. To be conservative we calculate 90% C.L. limits on the nucleon decay rates without making a background subtraction.

A summary of our present limits on various nucleon decay modes, arrived at by the methods described above, is given in Table II. We are in the process of searching for and setting limits on a wide variety of other modes as well.

Table II

90% C.L. Limits on Various Nucleon Decay Modes and $N\bar{N}$ Oscillation Rate From the IMB Detector (132 Days Live-time)

Mode	Hadron Nuclear Survival Probability	Background or Candidates	τ/B Limit(years)
$p \to e^+\pi^\circ$	.60	0	1.0×10^{32}
$p \to \mu^+\pi^\circ$	.60	0	1.0×10^{32}
$p \to \mu^+K^\circ$	.95	1	2.6×10^{31}
$N \to \nu K^\circ$	.95	3	0.8×10^{31}
$p \to e^+K^\circ$	.95	0	3.1×10^{31}
$N \to \bar{N}$ in oxygen	.60	3	2.4×10^{31}

Turning to the question of $N \to N$ oscillations in the oxygen nucleus we can use the fact that in general several pions will be created when the $\bar{N}$ annihilates and that these will show up as wide-angle events in the detector. A variable "isotropy angle" is defined to distinguish these events from the neutrino background events which predominantly produce light in only one hemisphere.

One starts with the best estimate of the vertex location of the event as determined by reconstruction techniques which make use of photon time-of-flight and the geometrical properties of Cherenkov light. Neutrino, nucleon decay, and $N\bar{N}$ events originating in the fiducial volume are approximately point sources of Cherenkov light in the detector. For multitrack events with significant light in more than a hemisphere the position and timing of the lit tubes are sufficient to locate the vertex to ~ 70 cm. Single track events require the additional constraint of the Cherenkov angle to achieve a comparable precision.

The recorded PMT hits are extrapolated to a sphere centered on this vertex, and an axis is found about which these hits would have the least moment of inertia, were they mass points. The hits are weighted by photoelectron count and inversely by absorption in the water. This axis is a good approximation to the true event axis for both single track and back-to-back two-track events.

A second axis is then found which points along the average direction of all the PMT hits, again weighted for the photoelectron and water absorption, as seen from the vertex. For single-track events this second axis is highly correlated to the first axis whereas for wide-angle multi-track events the two axes are uncorrelated. The "isotropy angle" is defined as the angle between the first and second axes.

In Figure 7 the event energy is plotted vs isotropy angle for the 109 data events. (The event energy E_C represents a lower limit on the energy released in the interaction, based on the assumption that all particles are showering and massless. The true energy of the event requires the addition ~ 250 MeV for each charged pion or muon in the event.) If the "isotropy angle"

and event energy are required to be greater than 20° and 500 MeV, respectively, then 50% of the simulated $N\bar{N}$ events are accepted and pass through the analysis chain. Three data events fall within these cuts. Monte Carlo simulations of the expected background from atmospheric neutrino interactions are consistent with the data on Figure 7. However, until this background is understood in more detail no background subtraction is made from the three events. Thus, with 6.7 events (90% C.L. upper limit) and a detection efficiency of 50% the lifetime limit is 2.4×10^{31} yr.

$$\tau(N \to \bar{N}) > \frac{(8.9 \times 10^{32} \text{ neutrons})\ (0.362 \text{ yr})\ (0.55 \times 0.9 \text{ efficiency})}{6.7 \text{ events (90\% C.L. limit)}}$$

$$= 2.4 \times 10^{31} \text{ yr.}$$

This result is also listed in Table II.

We conclude with a few remarks about the neutrino background. We have estimated the background by using neutrino interactions recorded in the Gargamelle bubble chamber at CERN. The chamber was filled with heavy freon (CF_3Br) and so the nuclear effects in water are approximately accounted for. This is important since pion scattering in the nucleus can increase the number of neutrino events with a large (> 150°) included angle between the pion and lepton, thereby mimicking proton decay. I would like to emphasize the importance of taking into account such nuclear interactions when searching for nucleon decay. Corrections are made to the Gargamelle data to account for the expected energy spectrum and electron neutrino rate for atmospheric neutrinos.

Using track identification and momenta from the Gargamelle data we have simulated 2.5 years of neutrino data in our detector an passed the events through our standard analysis procedures. If we plot these events using the variable of Figure 7, for example, the results appear to be entirely consistent with Figure 7. In particular there are 38 events in the region demarcated by the dotted line. Hence we expect 5.5 ± 2 events in that region on Figure 7. This is not inconsistent with the 3 ± 1.7 events that we see.

Of course individual events frequently contain more information than the two variables depicted on Figure 6 or Figure 7. In particular, for two-body modes the included angle and energy sharing between the two tracks can be significant in identifying the event as background or signal. Nevertheless, it appears that for certain hypothesized modes of proton decay and $N\bar{N}$ oscillations we are running into the neutrino induced background at a level of ~ 5×10^{31} yr.

CONCLUSIONS

-There appears to be no evidence for proton decay at the level of 10^{32} yrs for "easy" modes such as $e\pi^\circ$, $\mu\pi^\circ$, $e\eta^\circ$, $\mu\eta^\circ$, or at a level of a few times 10^{31} yrs for some of the "hard" modes involving K's, K^*'s, and/or neutrinos. The latter limit applies also to $N \to \bar{N}$ in oxygen.

-What about the future?

- The "easy" modes can be pushed another factor 3-5 by IMB before running into background.
- The "hard" modes can perhaps be pushed another factor of 5-10 but it will require a very detailed understanding of the background specific to a given detector. New detectors coming into operation that will be concentrating on this are: Kamiokande, Frejus, Kolar-N, HPW, IMB (upgraded?), and Soudan-2.

The rationale for believing that protons decay is still strong. We still have hope that someone will prove it within the next few years. Lacking that, one can perhaps conceive of a detector containing > 10,000 tons of free hydrogen. This would allow one to make very stringent requirements on the opening angle and energy sharing of two-body modes and thereby virtually eliminate the neutrino background. Such a detector could see proton decay at a level of 3×10^{33} yrs, or else set the limits there, in a few years of operation.

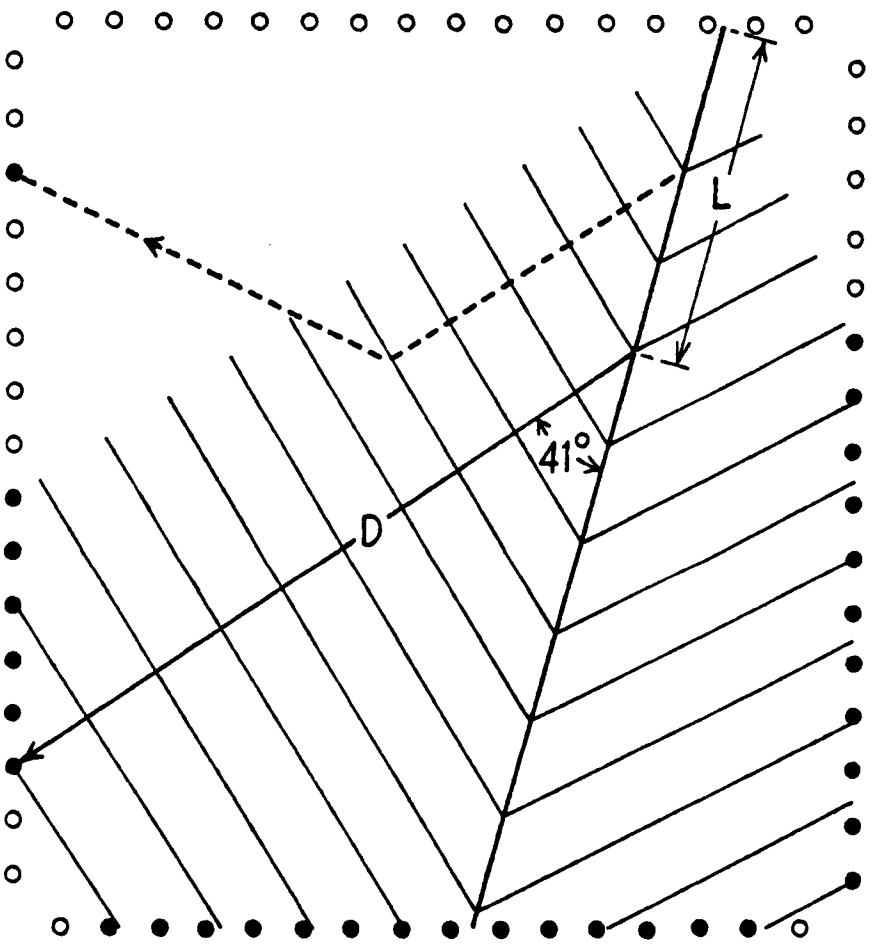

Figure 1

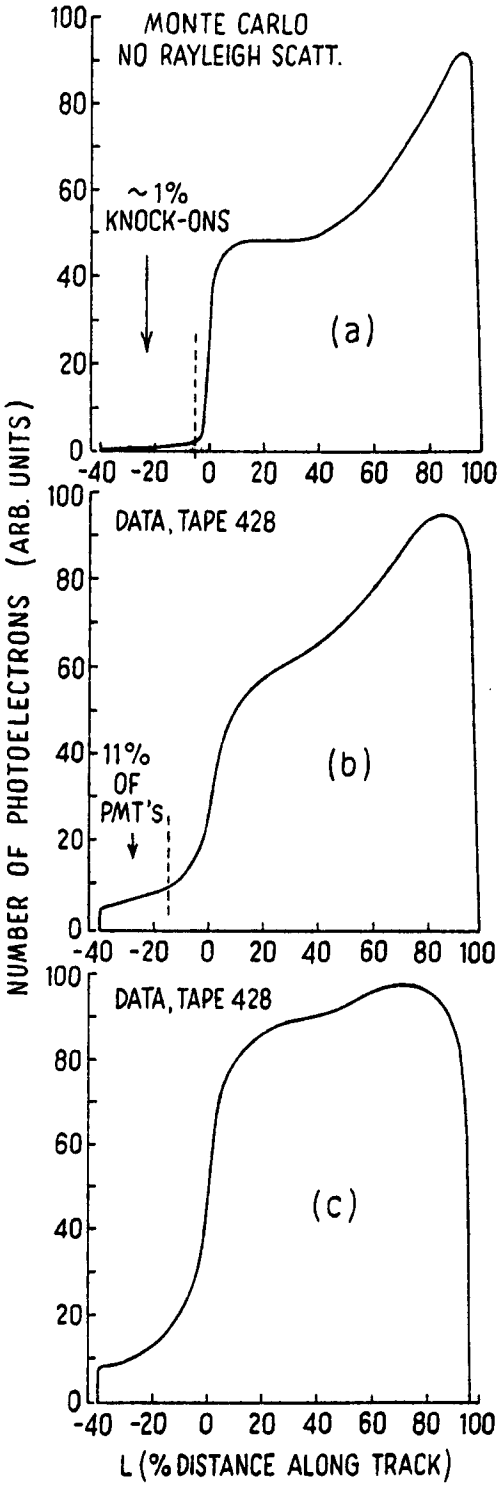
MONTE CARLO
NO RAYLEIGH SCATT.
~1%
KNOCK-ONS
(a)
DATA, TAPE 428
11%
OF
PMT'S
(b)
DATA, TAPE 428
(c)
NUMBER OF PHOTOELECTRONS (ARB. UNITS)
L (% DISTANCE ALONG TRACK)
100
80
60
40
20
0
-40 -20 0 20 40 60 80 100

Figure 2

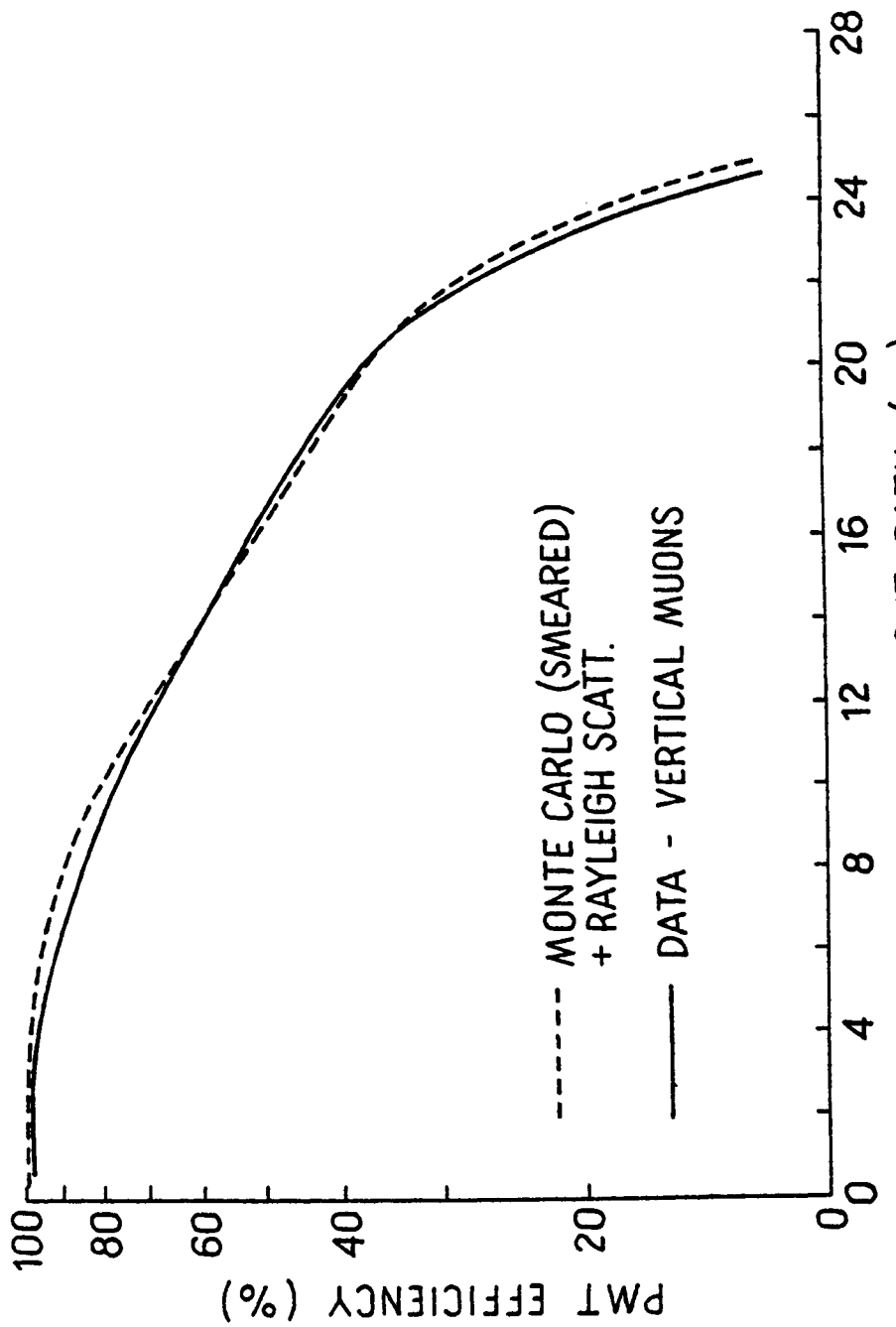
PMT EFFICIENCY (%)
100
80
60
40
20
0
0
4
8
12
16
20
24
28
PHOTON FLIGHT PATH (m)
MONTE CARLO (SMEARED)
+ RAYLEIGH SCATT.
DATA - VERTICAL MUONS

Figure 3

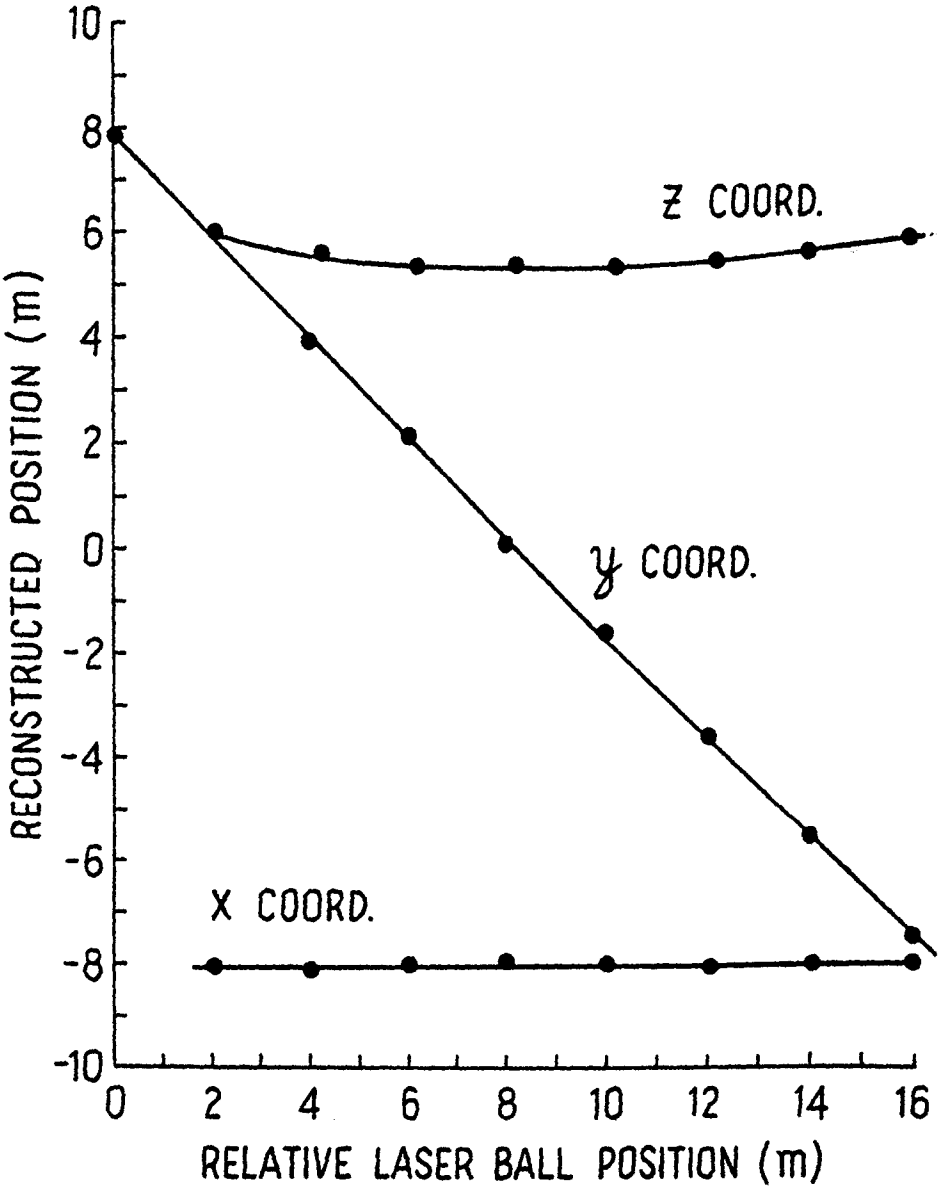
10
8
6
4
2
0
-2
-4
-6
-8
-10
RECONSTRUCTED POSITION (m)
Z COORD.
y COORD.
X COORD.
0
2
4
6
8
10
12
14
16
RELATIVE LASER BALL POSITION (m)

Figure 4

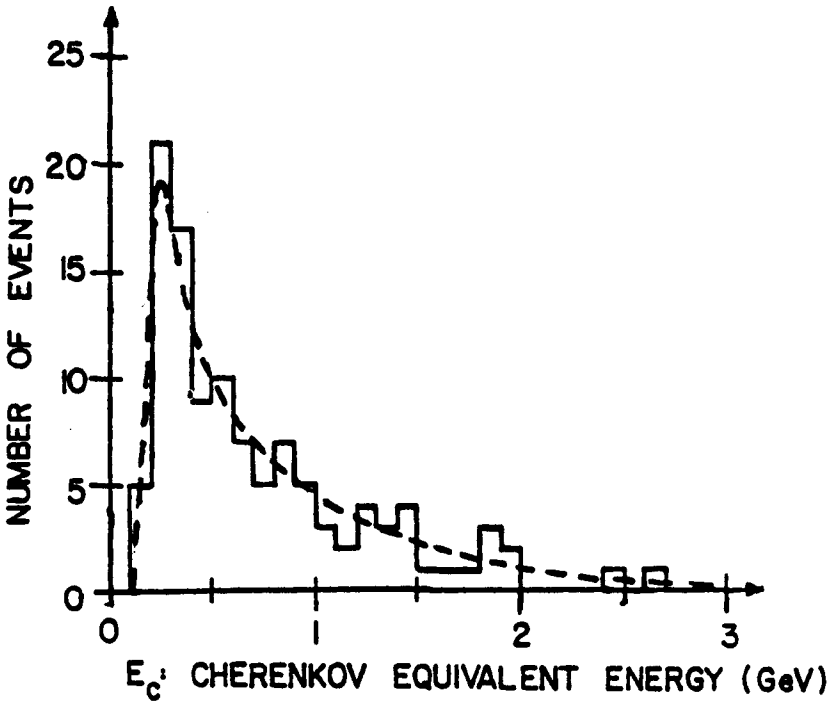
25
20
15
10
5
0
NUMBER OF EVENTS
0
1
2
3
E_c: CHERENKOV EQUIVALENT ENERGY (GeV)

FIGURE 5

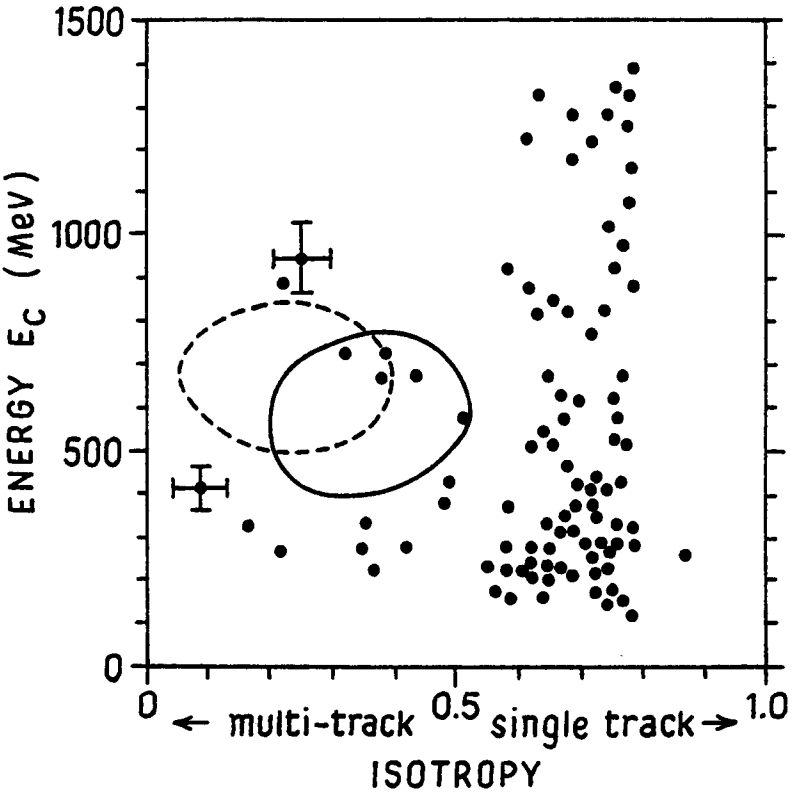
1500
1000
500
0
ENERGY E_C (MeV)
0
← multi-track
0.5
single track →
1.0
ISOTROPY

FIGURE 6

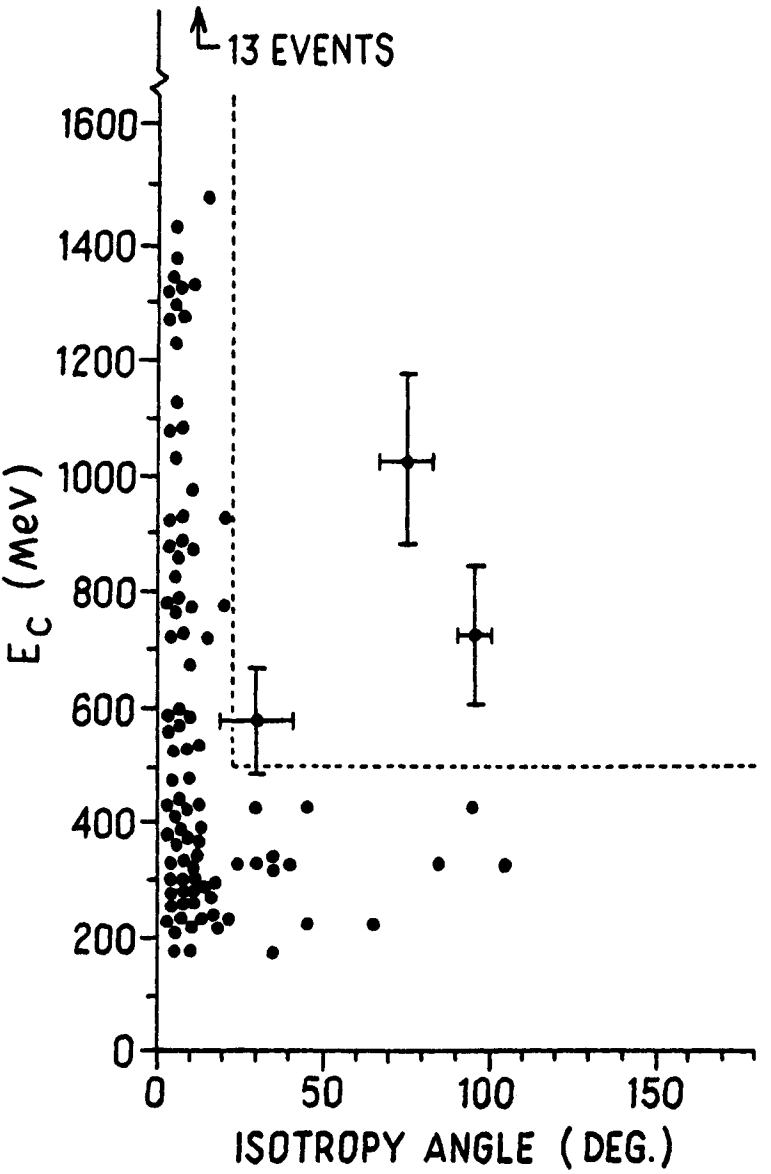
13 EVENTS
1600
1400
1200
1000
800
600
400
200
0
E_C (MeV)
0
50
100
150
ISOTROPY ANGLE (DEG.)

FIGURE 7